

DEPOSITION OF MICROCRYSTALLINE SILICON ONTO GLASS BY MICROWAVE PLASMA-ENHANCED SPUTTERING

P. Müller, W. M. Holber*, R. Gat*, W. Henrion, E. Nebauer**, V. Schlosser***, I. Sieber, and W. Fuhs
Hahn-Meitner-Institut, Rudower Chaussee 5, D-12489 Berlin, Germany, Tel. +49/30/67053310, eMail: mueller-p@hmi.de

*Applied Science and Technology, Inc., 35 Cabot Road, Woburn MA 01801, USA, Tel. +1/781/9335560

**Ferdinand-Braun-Institut für Höchstfrequenztechnik, Rudower Chaussee 5, D-12489 Berlin, Tel. +49/30/63922701

***Institut für Materialphysik, Universität Wien, Strudlhofgasse 4, A-1090 Wien, Tel. +43/1586/340927

ABSTRACT: To deposit Si in crystalline modification within reasonable times at temperatures ≤ 500 °C (stability limit of borosilicate glass) the reacting particles leading to layer growth have to be supplied with additional energy. For this reason the technique of microwave plasma-enhanced sputtering (MPES) has been applied to the deposition of undoped and P-doped Si. In the MPES method the target material is sputtered into a dense ECR plasma which causes the majority of the species depositing onto the substrate to consist of ions, rather than neutrals. The Si films were deposited with a rate of 10 nm/min at temperatures between 350-450 °C. In order to stimulate crystalline growth and to improve the quality of the films hydrogen has been added to the sputter gas Ar. Film inspection by SEM, measurement of the optical reflectance and transmittance (0.5-6 eV), Raman scattering, and thin film XRD confirmed the crystalline modification of the layers with an average crystallite size of 20-30 nm. Moreover the Si layers have been characterized by SIMS profiling (to trace H, C, O, Ar, Fe, and Cr), ESR ($1-2 \times 10^{17}$ dangling bond spins/cm³), and measurements of the dark conductivity and the Hall effect.

Keywords: Microcrystalline Si – 1: Sputtering – 2: Microwave plasma – 3

1. INTRODUCTION

The required reduction of material consumption, costs, and energy payback time in future photovoltaics will be possible if thin film technologies combined with low-temperature processing can be used for its production. With respect to the potential high-efficiency, long-term stability, non-toxicity, and the availability of the basic material crystalline silicon thin film solar cells are of special interest [1,2]. In order to reduce the expenses to 1 XEU/W_p, the cost of the substrates, however, must be less than 50 XEU/m² even if a module efficiency of 10 % can be assumed. In large scale production borosilicate floatglass with a thermal stability limit ≈ 500 °C can meet this target value [3]. In addition to costs glass has also advantages relating to its transparency, electrical insulation, chemical stability including weatherresistance, possibility of a matched thermal expansion coefficient, realization of light trapping, and easy recycling. But in comparison with low-cost multicrystalline Si substrates difficulties may arise with respect to the surface passivation at the glass/silicon interface [4]. A topical assessment of the applicability of glass as substrate for the growth of crystalline silicon films is given in [5].

A great variety of techniques has been applied to the preparation of crystalline Si layers on glass. These include e.g. PECVD [6], ECRCVD [7,8], hot wire CVD [9] or cat-CVD [10], sputtering [11], and special solution growth [12]. Modification of the layers often takes place by laser crystallization or by a prolonged solid phase crystallization. The manufacturing techniques have not only to meet the requirements with respect to adequate electronic properties of the Si layers as necessary for their application in solar cells or active-matrix thin film displays, but they must also enable (in principle) a large area deposition [13] and a processing within reasonable times (time for deposition and of layer modification). At present the realization of a sufficiently high deposition rate (desirable ≥ 100 nm/min) is one of the most serious problems in the low-temperature route of the development of crystalline Si thin film solar cells. The possibility of a fast deposition of $\mu\text{-Si:H}$ in the case of VHF-PECVD is shown in [14]. The higher

deposition rates obtained so far are connected with a considerable reduction of the material quality.

The present paper reports on the deposition of Si by microwave plasma-enhanced sputtering (MPES) which has been carried out with the goal of achieving a high Si growth rate in crystalline modification at temperatures compatible with borosilicate glass substrates. This technique, sometimes also described as high-density plasma vapor deposition (HDPVD), corresponds to a superposition of a DC or RF magnetron sputter process with the independent excitation of a dense plasma by microwave electron cyclotron resonance. This allows the possibility of independently controlling the flux and energy of the depositing species, while still achieving rates that are practical for manufacturing implementation. Moreover it can be performed at neutral gas pressures as low as 0.3 mTorr. The presence of the high-density plasma causes an increase of the sputter rate and a substantial ionisation of the sputtered particles whose additional but nevertheless moderate energy supply (low energy and large flux) will lead to increased surface mobility of the species contributing to layer growth.

Up to now MPES has been applied to the deposition of oxides, as e.g. SrTiO₃ [15,16] and SiO₂ [17,18], Si oxynitride [19], metals [20-22], and compounds such as TiN and hard coating materials. In the case of Cu (of interest for integrated circuit metallization) growth rates of 50-500 nm/min have been achieved. A review concerning the thin film deposition by microwave plasmas has been published in [23]. With the use of high-density plasma excitation MPES may allow some replacement of high-quality CVD processes by PVD processes with less technical efforts.

2. EXPERIMENTAL

The deposition system consists of the plasma source with the magnetron sputter setup (target diameter 125 mm) as an integral part and a larger chamber with the substrate chuck as shown in Fig. 1. The microwaves are launched

into the plasma source through a cylindrical quartz window and an annular gap between the source wall and the dark space shield of the sputter unit. The plasma evolves only at the end of this gap near the target surface. Thus due to its geometric position the microwave entrance window is not only protected from being coated but also shielded from interaction with the plasma. A dual electromagnet surrounds the target and provides the 875 Gauss required to achieve the ECR condition. The substrates are located at a distance of 30 cm from the target. The vacuum chamber is pumped by a 2200 l/s turbomolecular pump and the base pressure is lower than 1×10^{-7} Torr.

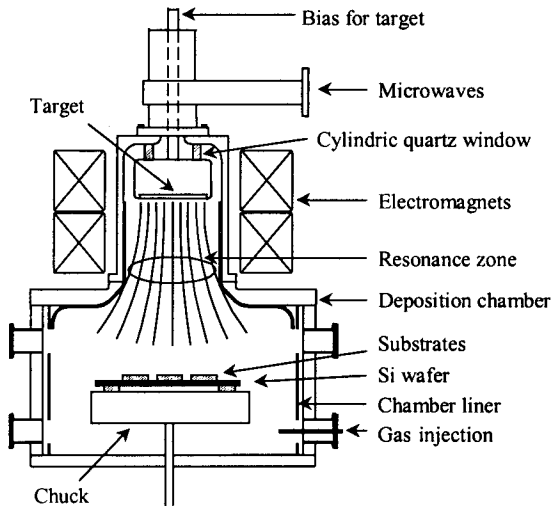


Figure 1: Cross-sectional view of the MPES system.

In the experiments performed so far the substrates (Corning glass 7740, Corning glass 1737, high-purity silica, and Si wafer) were thermally and electrically insulated from the chuck. Prior to deposition the substrates are heated to initial temperatures above 350 °C by plasma impact. During deposition, depending on the applied microwave power, a further temperature increase to a maximum value of about 450 °C (indicated by a pyrometer) has been reached. In order to stimulate crystalline growth up to 35 % hydrogen has been added to the sputter gas Ar. The total gas flow was adjusted to values ≤ 75 sccm leading to process pressures below 3 mTorr.

3. RESULTS AND DISCUSSION

3.1 Crystallinity

The crystalline modification of the Si layers was proved by SEM inspection, measurement of the optical reflectance and transmittance, Raman scattering, and XRD. Fig. 2 shows a SEM picture which exhibits the typical microcrystalline structure. On the fractional area of the film there are hints to columnar growth with preferred orientation of the grains. However, the columnar structure is much less pronounced than in $\mu\text{-Si}$ films deposited by PECVD. The average size of these grains amounts to ≈ 100 nm.

The dielectric response in crystalline silicon shows two distinct structures in the reflectivity spectrum at 3.4 eV (E_1) and at 4.55 eV (E_2) as well as a shoulder at about 5.4 eV (E_3) (cf. Fig. 3). These interband structures are due to the critical points of the electronic band structure and are sensitive to imperfect crystallinity [24,25]. The variations

of E_1 and E_2 with crystallite size have opposite signs (cf. Fig.3 for $\mu\text{-Si}$) and are shifted to a middle peak position for the limiting case of amorphous Si [24]. The correlation of our optical spectra for the $\mu\text{-Si}$ film with crystal size effects determined from x-ray results gives a crystallite size of about 20 nm.

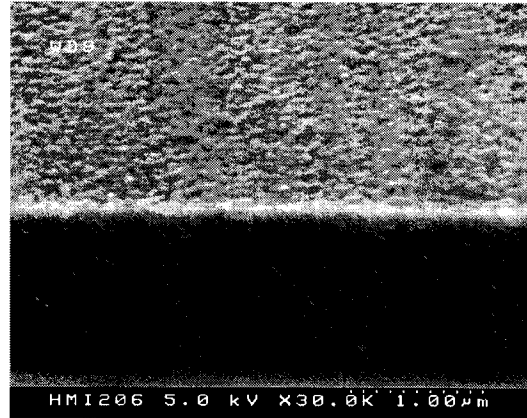


Figure 2: SEM picture of a 1.1 μm thick nominally undoped Si layer deposited onto Corning glass 7740.

From the analysis of the transmission and reflectivity spectra in the near infrared interference region we obtained for the film shown in Fig. 2 a thickness of 1.17 μm , a surface roughness of 7 nm, a space filling of 0.95 and the refractive index n as well as the absorption index k . The extrapolated static values for the monocrystalline wafer and the microcrystalline sample are 3.417 and 3.143, respectively, that means a density reduction of 8 %. The reduced density is the reason for the reduced refractive index and the measured reflectivity decrease in the interband region.

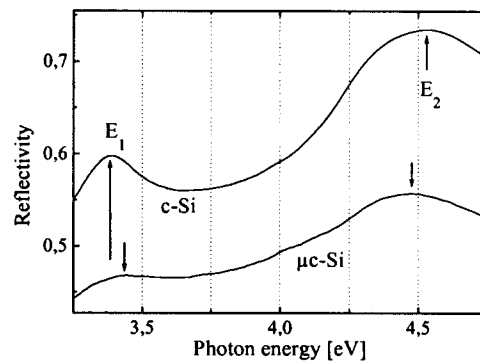


Figure 3: Reflectivity spectra of $\mu\text{-Si:H}$ deposited on Corning glass 7740 and of monocrystalline Si taken at 295 K.

Raman spectra have been taken in order to further examine the crystallinity of the layers. The measurements were performed with a DILOR-XY-spectrometer equipped with a microscope (Olympus BH2) in combination with an Ar laser (excitation wavelength 514.5 nm) whose penetration depth into Si corresponds to ≈ 1 μm . The laser power of 2.5 mW leads to an excitation density of 26.5 kW/cm^2 in the 2 μm measuring spot. Fig. 4 shows the Raman spectrum of a 1.1 μm thick undoped Si film with the morphology as shown in Fig. 2. The obtained signal is clearly dominated by the intensive Raman-active TO mode which is located at 519.5 cm^{-1} in the case of monocrystalline Si. The signal in Fig. 4 can be considered as a

superposition of a small peak near 480 cm^{-1} as typical for amorphous Si, a main Raman peak which distinguishes from that of monocrystalline Si only by a minor line broadening and a negligible shift to lower wave numbers, and an intermediate signal at about 500 cm^{-1} which is due to the contribution of the grain boundaries. This interpretation is supported by comparative measurements from the

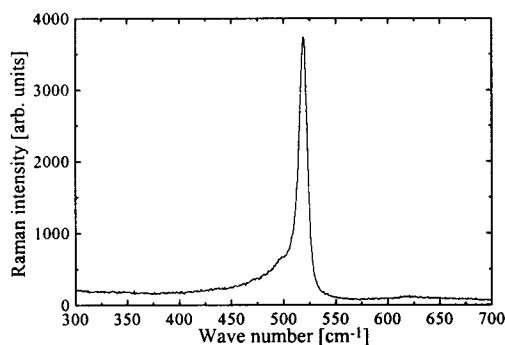


Figure 4: Raman spectrum measured on a $1.1\ \mu\text{m}$ thick undoped Si layer deposited onto Corning glass 7740.

back side (through the substrates), on uncoated glass substrates, and on monocrystalline bulk Si as well as on amorphous Si layers. The spectrum of Fig. 4 is quite similar to that of optimized $\mu\text{c-Si:H}$ from PECVD with a crystallinity above 85 %.

Fig. 5 shows the results of thin film x-ray diffraction on a $1\ \mu\text{m}$ thick undoped Si layer deposited onto Corning glass 7740. The measurements were performed with a Philips X'Pert diffractometer using $\text{CuK}\alpha$ radiation and an incidence angle of 3° . Under these conditions the penetration depth of the x-rays into Si corresponds to about $3\ \mu\text{m}$. Thus the diffractogram (full line) represents a superposition of the signal caused by the Si layer and the contribution of the substrate. In order to visualize the

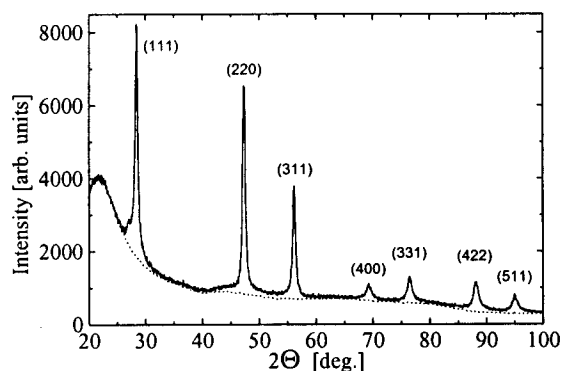


Figure 5: $I(2\theta)$ -diffractogram of a $1\ \mu\text{m}$ thick undoped Si layer deposited onto borosilicate glass (full line) in comparison with the contribution of the substrate to the signal (dotted line).

background signal the measured (and smoothed) diffractogram of the glass substrate is shown in addition. This curve was multiplied by the factor 0.70 (dotted line) which results from the absorption of the primary beam as well as of the diffracted x-rays within the Si layer. Compared with the ratio of peak heights to be expected in the case of randomly oriented crystallites the (220) and the (311) signal are increased by a factor 1.71 and 1.67, respectively.

Hence the diffractogram in Fig. 5 suggests a slight preference of these orientations during the growth. The trace of a small satellite signal on the low angle side of the (111) and of the (220) peak may be a hint to polytypism in the grains (presence of microtwins) [26,27]. An evaluation of the FWHM value of the (220) peak according to simple Scherrer analysis leads to a mean crystallite size of $30\ \text{nm}$ (crystallites oriented normal to the surface). On the other hand the plane view SEM inspection of the Si layer indicates a structure parameter (diameter of grains) of about $100\ \text{nm}$. A comparison of both results clearly confirms the fact that the structures observed by SEM (cf. Fig. 2) are composed by smaller crystallites. This feature is typical for $\mu\text{c-Si}$ films.

3.2 SIMS, ESR, and Electrical Characterization

SIMS profiling suggests an unusually high oxygen concentration of up to $1 \times 10^{21}\ \text{cm}^{-3}$ which most probably resulted from the insufficient purity of the process gas. Hydrogen and carbon followed with concentrations up to $2 \times 10^{20}\ \text{cm}^{-3}$ and up to $2 \times 10^{19}\ \text{cm}^{-3}$, respectively. Despite careful investigation an incorporation of Ar in the layers could not be detected. Contaminations of Fe and Cr were below $2 \times 10^{16}\ \text{cm}^{-3}$. The results of SIMS clearly indicate the necessity of reducing oxygen (and carbon) contamination during the sputter process.

ESR measurements on undoped Si layers deposited onto high-purity silica and Corning glass 7740 led to dangling bond spin densities of $1\text{--}2 \times 10^{17}\ \text{cm}^{-3}$. These values should likewise be improved by a better contamination control (and possibly by a layer posttreatment).

Dark conductivity and magnetotransport measurements have been carried out with varying magnetic fields in the van der Pauw geometry at $T = 294\ \text{K}$. In order to exclude magnetoresistance effects the data were evaluated by a second order fit. In the case of a $1\ \text{cm}^2$ sample prepared in the same deposition run as the layer shown in Fig. 2 a sheet resistance of $1.18 \times 10^9\ \Omega/\text{square}$ and a Hall coefficient R_H/d of $-3.28 \times 10^5\ \Omega/\text{T}$ were obtained. Assuming a sample thickness of $1.1\ \mu\text{m}$ and a scattering factor of 1 this led to a conductivity of $7.7 \times 10^{-6}\ \Omega^{-1}\text{cm}^{-1}$, an electron concentration of $1.7 \times 10^{13}\ \text{cm}^{-3}$, and a Hall mobility of $2.8\ \text{cm}^2\text{V}^{-1}\text{s}^{-1}$.

The results of the layer characterization confirm that by virtue of the additional supply of plasma energy MPES allows one to grow crystalline Si on glass at temperatures of only about $400\ ^\circ\text{C}$. To our knowledge these experiments represent the first example of Si deposition by ECR sputtering. The measured deposition rates of only about $10\ \text{nm}/\text{min}$ were, however, much smaller than to be expected according to previous runs with Cu, Al and TiN in the same system. In those investigations Cu and Al were deposited at rates $>300\ \text{nm}/\text{min}$ with excellent homogeneity on $200\ \text{mm}$ substrates.

4. OUTLOOK

In future application of MPES to Si deposition an improvement of the experimental conditions as well as an optimization of the process parameters are required. The possible improvements of the experimental conditions refer to a further reduction of the base pressure (to lower the contamination by plasma-activated residual gas particles as e.g. oxygen), use of a sputter-up arrangement (to avoid particulates on the layer), installation of a shutter (to allow

presputtering), heating of the substrates by a heatable chuck (to determine the deposition temperature), and the application of a definite RF or DC bias (to adjust the bombarding energy of the charged particles impinging on e.g. metal- or TCO-coated glass substrates). The optimization of process parameters concerns (besides other conditions) the determination of an appropriate substrate temperature, a suitable bias voltage, possible pulse time modulation of the plasma [28], and an optimum hydrogen concentration in the sputter gas. The latter should lead to dense layers [8] while maintaining a maximum growth rate by realization of a reasonable equilibrium between Si deposition and preferential etching of weakly bound Si. Special attention must be directed to differences between the doping concentration in the target and in the layer due to the formation and desorption of volatile compounds of phosphorus and boron [29].

Compared with other ion-assisted deposition techniques as e.g. ECR-CVD [30] or the ion-assisted evaporation process described in [31] MPES should likewise allow low-temperature homoepitaxy (or even selective epitaxy [32]) of Si. Furthermore due to the very high flux of activated particles with nevertheless moderate energy there seem to be good opportunities to achieve epitaxial-like growth on Si seed layers. In this way MPES may enable low-temperature preparation of large grain size Si multilayer structures as required for thin film cells with efficiencies $\geq 10\%$.

ACKNOWLEDGEMENTS

The authors are indebted to Dr. K.-W. Brzezinka of the Bundesanstalt für Materialforschung und -prüfung for measurements of the Raman spectra. Furthermore they like to thank P. Kanschä for performing the ESR measurements. This work was supported by the European Commission under the CRYSTAL project.

REFERENCES

- [1] J. H. Werner, R. Bergmann, and R. Brendel, in *Advances in Solid State Physics*, Vol. 34, Ed. R. Helbig, Vieweg, Braunschweig 1994, p.115.
- [2] S. R. Wenham and M. A. Green, *Progr. Photovolt.* **4** (1996) 3.
- [3] Borofloat® glass, product information, Schott Jenaer Glaswerk GmbH, 1997.
- [4] A. W. Blakers, *Solar Energy Mater. Solar Cells*, **51** (1998) 385.
- [5] R. B. Bergmann, J. Köhler, R. Dassow, C. Zaczek, and J. H. Werner, *phys. stat. sol. (a)* **166** (1998) 587.
- [6] M. Tzolov, F. Finger, R. Carius, and P. Hapke, *J. Appl. Phys.* **81** (1997) 7376.
- [7] P. Müller, I. Beckers, E. Conrad, L. Elstner, W. Fuhs, *Proceed. 25th IEEE PVSC* (1996) p.673.
- [8] B. Sanghoon, A. K. Kalkan, C. Shangcong, and S. J. Fonash, *J. Vac. Sci. Technol. A* **16** (1998) 1912.
- [9] J. Guillet, A. R. Middy, J. Huc, J. Perrin, B. Equer, and J. E. Bourée, *Proceed. 14th PVSEC*, H. S. Stephens & Ass., Bedford, UK, 1997, p. 1475.
- [10] R. Iiduka, A. Heya, and H. Matsumura, *Solar Energy Mater. Solar Cells*, **48** (1997) 279.
- [11] Y. Mishima, M. Takei, T. Uematsu, N. Matsumoto, T. Kakehi, U. Wakino, and M. Okabe, *J. Appl. Phys.* **78** (1995) 217.
- [12] T. Boeck, Th. Teubner, K. Schmidt, and P.-M. Wilde, *J. Cryst. Growth*, *Proceed. ICCG-12/ICVGE-10*, Jerusalem, 1998, to be published.
- [13] J. Pelletier and T. Lagarde, *Thin Solid Films* **241** (1994) 240.
- [14] P. Torres, H. Keppner, J. Meier, U. Kroll, N. Beck, and A. Shah, *phys. stat. sol. (a)* **163** (1997) R9.
- [15] M. Itsumi, S. Ohfuji, and H. Akiya, *Jpn. J. Appl. Phys.* **35** (1996) 4963.
- [16] K. Ikuta, M. Tsukada, H. Nishimura, *Jpn. J. Appl. Phys.* **37** (1998) 1960.
- [17] M. Matsuoka and S. Tohno, *J. Vac. Sci. Technol. A* **13** (1995) 2427.
- [18] D. W. Gao, Y. Kashiwazaki, K. Muraoka, H. Nakashima, K. Furukawa, Y. C. Liu, K. Shibata, and T. Tsurushima, *J. Appl. Phys.* **82** (1997) 5680.
- [19] D. W. Gao, Y. Kashiwazaki, K. Muraoka, H. Nakashima, K. Furukawa, Y. C. Liu, and T. Tsurushima, *Jpn. J. Appl. Phys.* **36** (1997) L 1692.
- [20] L. A. Berry and S. M. Gorbalkin, *J. Vac. Sci. Technol. A* **13** (1995) 343.
- [21] Y. Yoshida, *Plasma Sources Sci. Techn.* **5** (1996) 275.
- [22] M. Delaunay and E. Touchais, *Rev. Sci. Instrum.* **69** (1998) 2320.
- [23] J. Musil, *Vacuum* **47** (1996) 145.
- [24] W. Henrion, R. Krankenhagen, M. Schmidt, I. Sieber, and H. Flietner, *Solid State Phenom.*, **37-38** (1994), 387.
- [25] E. Bardet, J. E. Bourée, M. Cuniot, J. Dixmier, P. Elkaim, J. Leduigou, A. R. Middy, and J. Perrin, *J. Non-Cryst. Solids* **198-200** (1996) 867.
- [26] R. Nozawa, H. Takeda, M. Ito, M. Hori, and T. Goto, *J. Appl. Phys.* **81** (1997) 8035.
- [27] J. Dixmier, private communication.
- [28] S. Samukawa, H. Ohtake, and T. Mieno, *J. Vac. Sci. Technol. A* **14** (1996) 3049.
- [29] M. Cuniot, private communication.
- [30] E. Conrad, L. Elstner, W. Fuhs, W. Henrion, P. Müller, B. Selle, and U. Zeimer, *Proceed. 26th IEEE PVSC* (1997) p.755.
- [31] R. Bergmann, C. Zaczek, N. Jensen, S. Oelting, and J. Werner, *Appl. Phys. Lett.* **72** (1998) 2997.
- [32] K. Sasaki and T. Takada, *Jpn. J. Appl. Phys.* **37** (1998) 402.